

# Non-Raster Sampling in Atomic Force Microscopy: A Compressed Sensing Approach

Sean B. Andersson  
Department of Mechanical Engineering and  
Division of Systems Engineering  
Boston University  
Boston, MA 02215 USA  
sanderss@bu.edu

Lucy Y. Pao  
Department of Electrical, Computer, and  
Energy Engineering  
University of Colorado Boulder  
Boulder, CO 80309 USA  
pao@colorado.edu

**Abstract**—Atomic force microscopy is a powerful tool that has had a tremendous impact in understanding systems with nanometer-scale features. In this work we explore the use of compressed sensing as a means of sampling data and generating an image. Under this approach only a small number of the pixels in an image, typically as few as 10%, need to be sampled to generate an accurate image. We show that when combined with time-optimal control to move the tip of the microscope between measurement locations, the imaging time is comparable to high-speed AFM systems while also greatly reducing the interactions with and force applied to the sample. In addition, the approach can significantly reduce the imaging time in applications such as force mapping in which the tip is moved point-by-point through a sequence of measurement locations rather than continuously scanned as in standard imaging.

## I. INTRODUCTION

One of the enduring challenges in atomic force microscopy (AFM) is its poor temporal resolution relative to the rate of dynamics in many systems of interest [1]. Most commercial instruments still take on the order of seconds to minutes to produce a single image, depending on the quality, image size, and other factors. In addition, because the tip applies a (small) force to the sample, sample damage and modification of the natural process being studied are of constant concern, especially when imaging soft biological samples. As a result, there are a variety of ongoing efforts aimed at improving the imaging rate and sensitivity of the instrument [2].

Approaches to high speed AFM can be broadly categorized into two branches. The first targets the hardware, using, for example, small cantilevers [3], novel actuator designs [4], [5], and alternative drive mechanisms [6]. The second targets the controllers and algorithms, using, for example, a combination of feedforward and feedback control [7], [8], robust controllers [9], and iterative control schemes [10]. Under all these methods, images are built pixel-by-pixel by raster scanning the tip across the sample. They aim to speed up the imaging process by moving the tip of the AFM faster without sacrificing image quality.

Recently, an entirely different approach to improving the imaging rate in AFM has been introduced by one of the authors [11]. The fundamental idea is to replace the raster-scan with a feedback law driving the tip to acquire measurements only from regions of interest. Imaging time is improved by reducing the amount of sampling rather than increasing

the scan rate. Work to date has focused on samples which are string-like in nature, such as biopolymers (e.g., DNA, actin, microtubules), cell boundaries, or crystal edges. Taking advantage of the structure of such samples, we designed an approach called *local raster scanning* which dithers the tip back and forth across the sample, tracking the sample along its length. All measurements are then near the sample, and improvements in the imaging rate by an order of magnitude or better are possible.

The main drawback of the local raster-scan scheme is that it can be used only on string-like samples. Further, its improvement over a standard raster scan becomes less pronounced the more a sample “fills” the image. In this paper, we describe a *global* non-raster scheme. This scheme takes advantage of the fact that most images are compressible. Using the theory of compressed sensing (CS) [12], an accurate image can be reconstructed based on a small collection of measurements.

The application of CS to improve the imaging rate in AFM has recently been independently proposed in [13]. In that work, a series of rectangles was scanned and the full image reconstructed from the small data set. Such a regular scan pattern, however, has a low probability of satisfying the requirements for good reconstruction based on CS theory. Related ideas have also been proposed in the context of surface metrology [14] as well as adaptive sampling methods in AFM based on fractal compression [15].

Here we focus on a *random* pattern of sampling combined, guided by the theorems of CS, with minimum-time control to move the tip rapidly between measurement locations. We also briefly discuss the results when a continuous spiral scan pattern is used, similar to that in [13].

## II. OVERVIEW OF COMPRESSED SENSING

There are several good tutorials and overviews of CS in the literature, including [12], [16], [17]. We give here a brief overview sufficient to motivate our approach and refer the interested reader to those sources for more information.

Consider a discrete signal  $x \in \mathbb{R}^n$ . If the underlying signal is an image, as in the AFM application, string the pixels into a single  $n \times 1$  vector first. Let  $\Psi = [\psi_1 \psi_2 \cdots \psi_n]$  be an orthonormal basis for  $\mathbb{R}^n$  such that  $x$  can be expressed as

$$x = \Psi q \quad (1)$$

where  $q$  is the vector of weighting coefficients given by  $q_i = \langle x, \psi_i \rangle$ .

The signal  $x$  is said to be  $k$ -sparse if only  $k$  of the elements of  $q$  are non-zero. In practice, few real signals are truly sparse. Many however, are approximately sparse or *compressible*, such that only a few elements in  $q$  are significant. Given a signal  $x$ , it has been shown that the  $k$ -sparse approximation  $\hat{x}$  that minimizes the error

$$\|x - \hat{x}\|_p$$

for any  $\ell_p$  norm is the one given by thresholding, that is retaining just the  $k$  largest elements [18].

Under standard data acquisition, the full  $n$ -sample signal  $x$  is first acquired. It is then compressed by calculating the basis coefficients and then storing only the  $k$  largest. The fundamental idea of CS is to directly acquire a compressed signal without first sampling the full set of  $n$  samples. The challenge, of course, is that the location of the significant coefficients is not known *a priori*. Surprisingly, despite this, it is possible to produce an accurate, even exact, reconstruction of the original signal using far fewer than  $n$  measurements.

#### A. Measurement acquisition

Consider a collection of  $m \ll n$  linear measurements acquired by taking the inner product between the signal and a test vector,  $y_j = \langle x, \phi_j \rangle$ . Defining the measurement matrix  $\Phi = [\phi_1 \phi_2 \dots \phi_m]^T$ , the measurements can be written as

$$y = \Phi x = \Phi \Psi q \triangleq Aq. \quad (2)$$

Note that the process is non-adaptive; the measurement matrix is selected beforehand and remains fixed. To ensure the  $m$  measurements contain sufficient information about the sparse (or compressible) signal to enable its accurate reconstruction,  $\Phi$  should be *incoherent* with respect to the chosen basis  $\Psi$ . In essence, this means that the rows of  $\Phi$  cannot sparsely represent the columns of  $\Psi$  and vice versa. (A related condition is that the combined matrix  $A$  should have the *restricted isometry property* (RIP) [19].) One interesting feature of CS is that choosing  $\Phi$  as a random matrix from a suitable distribution (e.g., choosing each entry according to a uniform Bernoulli distribution or a zero-mean,  $1/n$ -variance Gaussian distribution [20]) ensures incoherence (and RIP) with high probability.

#### B. Signal reconstruction

The reconstruction of the signal  $x$  from the measurements  $y$  is achieved by solving a nonlinear optimization problem. It has been shown that under appropriate assumptions, the solution to the  $\ell_1$  optimization problem

$$\hat{q} = \arg \min \|q\|_1 \quad \text{subject to} \quad Aq = y \quad (3)$$

will exactly reconstruct a  $k$ -sparse vector and well approximate a compressible vector using  $O(k \log(n/k))$  measurements. This convex optimization problem can be solved using a variety of different algorithms, including basis pursuit and greedy, stochastic, and variational algorithms [16].

In the presence of noise, it makes sense to relax the constraints somewhat. In that setting, a common approach is to solve the optimization problem given by

$$\hat{q} = \arg \min \|q\|_1 \quad \text{subject to} \quad \|y - Aq\|_2 < \varepsilon \quad (4)$$

where  $\varepsilon$  is a user-defined parameter establishing an upper limit on the magnitude of the noise. This is once again a convex programming problem that can be solved by a variety of techniques.

If the underlying data set represents an image, one often uses a variant of the  $\ell_1$  minimization which relies on the fact that typically the gradient in an image is sparse. In that setting one defines a gradient operator  $D_{ij}$  on each pixel and then solves the problem

$$\hat{q} = \arg \min \sum_{i,j} \|D_{ij}q\|_2 \quad \text{subject to} \quad Aq = y. \quad (5)$$

As before, this problem can be modified to account for noise by relaxing the constraints as in (4).

### III. ACCURATE AFM IMAGES WITH LESS SAMPLING

One of the challenges in applying CS to the AFM imaging application is the fact that the sensor in the instrument, namely the tip, is essentially capable only of measuring a single point at a time. This directly translates into each row of the measurement matrix  $\Phi$  consisting of all zeros except for a single one at the pixel to be sampled. Note that is true even when scanning continuously across multiple pixels; due to the point-like nature of the tip, each pixel can be viewed as a single measurement even when taken in a single scan.

In this work, then, a measurement matrix is determined by selecting at random a small number (typically 10% to 20% of the total) to measure. A traveling salesman problem is then solved to determine the sequence through which to visit those pixels to minimize the total path length. Note that this is done offline and is independent on the sample (since as noted in Sec. II-A the measurements are non-adaptive). Motion between the points is then achieved using a robust time-optimal controller [21]–[23]. At each point, the tip is brought down until it contacts the sample, the height is measured, and it is then retracted and moved to the next point in the sequence. Once all measurements are collected, the image is reconstructed by solving one of the  $\ell_1$  optimization problems described in Sec. II-B.

While one of the motivations for alternative scan techniques is the desire to reduce the time it takes to acquire an image, the rough calculation described below shows that, due to the need to stop motion in the  $x$ - $y$  direction to engage and then withdraw the tip in the  $z$  direction at every sample location, the acquisition time is approximately the same as ‘fast’ raster scan methods that have been reported in the literature on commercial AFMs [24], [25]. Since the CS approach uses far fewer measurements, and since the approach to the sample can be finely controlled, the interaction with the sample is drastically reduced.

Commercially available AFMs typically have raster scan rates in the range of 1 Hz to 10 Hz, depending upon the

sample size, imaging resolution desired, and other factors. Using more advanced controllers on available commercial AFMs has shown that raster scan rates of over 100 Hz are achievable [24], [25]. Thus, a  $128 \times 128$  pixel image would take 128 s to 12.8 s to acquire using commercially available AFMs, and it would only take 1.28 s to acquire using AFMs that are on the horizon equipped with more advanced controllers.

The imaging time when using a smaller number (10% to 20%) of samples can be computed approximately as follows:

$$t_{\text{samples}} = m \times (t_{z_{\text{up}}} + t_{xy} + t_{z_{\text{down}}} + t_{\text{meas}}). \quad (6)$$

Here,  $m$  is the number of points measured,  $t_{z_{\text{up}}}$  is the average time needed to move the AFM tip away from the sample in the  $z$  direction after each measurement,  $t_{xy}$  is the average time to move to the next (pre-selected) measurement point,  $t_{z_{\text{down}}}$  is the average time needed to move the AFM tip to the sample in the  $z$  direction before each measurement, and  $t_{\text{meas}}$  is the time needed to measure the height at each point.

How large  $t_{z_{\text{up}}}$  is depends upon the expected sample topology. Using a 1st-order fit to the identified transfer function model of the  $z$ -direction dynamics of a piezoelectric tube scanner in [26] yields

$$G_z(s) = \frac{g}{s+a}$$

where  $g = 4.5127 \times 10^5$  and  $a = 1.5534 \times 10^4$ . This 1st-order fit provides a good match to the measured dynamics up to approximately  $10^4$  rad/sec. The time-optimal rest-to-rest motion control for this 1st-order system can be easily computed [27] to consist of one pulse that leads to a maneuver time of

$$t_{z_{\text{up}}} = \frac{-1}{a} \ln \left( \frac{1}{1 + \frac{a|z_0|}{g}} \right),$$

where  $|z_0|$  is the distance moved. This leads to a  $t_{z_{\text{up}}}$  of 2 to  $150 \mu\text{s}$  for motions of 1 nm to 250 nm in the  $z$ -direction.

After lifting the tip off the sample in a time  $t_{z_{\text{up}}}$ , we also assume a time-optimal motion in the  $x$ - $y$  direction to the next measurement point. A simplified 2nd-order fit to the identified transfer function model for the  $x$ -direction dynamics of an AFM  $x$ - $y$  stage [24] is

$$G_x(s) = \frac{K}{s^2 + 2\zeta\omega s + \omega^2},$$

where  $K = 1.8276 \times 10^7$ ,  $\omega = 2\pi(3.175 \times 10^2) = 1.9949 \times 10^3$  rad/s and  $\zeta = 0.6402$ . This 2nd-order fit provides a good match to the measured dynamics up to approximately  $2 \times 10^3$  rad/sec. For this AFM  $x$ - $y$  stage, the  $y$  direction has similar dynamics that are relatively decoupled to the  $x$  direction. The time-optimal control for a 2nd-order system with complex conjugate poles can be computed as discussed in [23]. As a result, the minimum maneuver time  $t_{xy}$  can be upper bounded by 4.1 ms and 1 ms for moves of less than 15.7 and  $1 \mu\text{m}$ , respectively.

The average  $t_{z_{\text{down}}}$  time is necessarily greater than the average  $t_{z_{\text{up}}}$  time since care must be taken to approach and

detect contact carefully so as not to damage the sample (or the AFM tip). Here, we will assume that the average  $t_{z_{\text{down}}}$  is 5 times  $t_{z_{\text{up}}}$ . Finally,  $t_{\text{meas}} = 0.5$  ms is a sufficient amount of time to measure the height at each measurement point.

In Sec. IV, we apply the CS approach to two samples, a grating and DNA. For the grating sample considered in Fig. 1, we then have

$$\begin{aligned} t_{z_{\text{up}}} &\approx 150 \mu\text{s} && \text{for 250 nm motion up in } z, \\ t_{xy10} &\approx 1.25 \text{ ms} && \text{for } 1.5 \mu\text{m average motions in } x\text{-}y \\ &&& \text{for 10\% sampling,} \\ t_{xy20} &\approx 0.8 \text{ ms} && \text{for } 0.75 \mu\text{m average motions in } x\text{-}y \\ &&& \text{for 20\% sampling,} \\ t_{z_{\text{down}}} &\approx 750 \mu\text{s}. \end{aligned}$$

Hence, when the image is  $128 \times 128$  pixels, applying (6) for 10% sampling (or 1,638 samples) and 20% sampling (or 3,277 samples), we have

$$t_{10\% \text{ samples, grating}} \approx 4.34 \text{ s}$$

and

$$t_{20\% \text{ samples, grating}} \approx 7.21 \text{ s}.$$

For the DNA sample considered in Fig. 3, we would then have:

$$\begin{aligned} t_{z_{\text{up}}} &\approx 2 \mu\text{s} && \text{for 1 nm motion up in } z \\ t_{xy10} &\approx 0.1 \text{ ms} && \text{for 25 nm average motions in } x\text{-}y \\ &&& \text{for 10\% sampling} \\ t_{xy20} &\approx 0.09 \text{ ms} && \text{for 12.5 nm average motions in } x\text{-}y \\ &&& \text{for 20\% sampling} \\ t_{z_{\text{down}}} &\approx 10 \mu\text{s} \end{aligned}$$

Again, applying (6) for 10% and 20% sampling of a  $128 \times 128$  pixel image yields

$$t_{10\% \text{ samples, DNA}} \approx 1.00 \text{ s}$$

and

$$t_{20\% \text{ samples, DNA}} \approx 1.97 \text{ s}.$$

While these are only approximate calculations, they show that the imaging time when using the 10% to 20% sampling approach is comparable and will likely not be shorter than ‘fast’ raster scan methods that have been achieved in many research labs. The primary benefit of the reduced sampling approach, then, is minimizing the interaction with the sample. In the standard raster scan, the tip essentially interacts with the sample everywhere. Further, even in tapping mode the instrument applies shear forces that make imaging soft samples challenging and that can damage fragile samples. Under this scheme, there are no lateral forces applied as the tip is brought directly down upon the sample. Further, the approach phase can be carefully controlled to minimize the applied normal force.

The CS scheme can also be applied directly to other imaging applications in AFM, including force mapping and

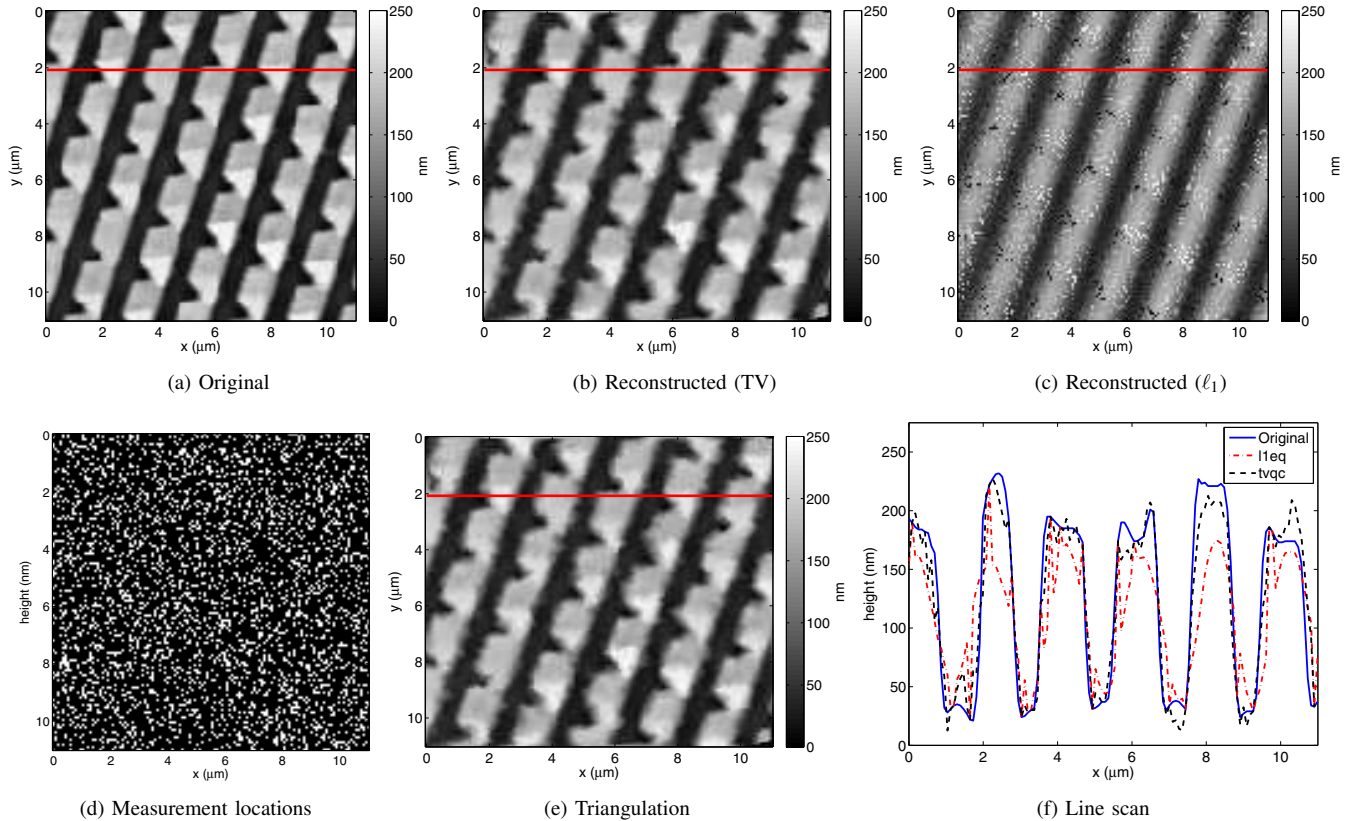


Fig. 1. Grating sample results using 20% of the pixels. (a) The full raster-scan image is filled with the regular pattern of the grating. (b) Reconstruction using the relaxed TV optimization problem (see Sec. II-B). (c) Reconstruction using the relaxed  $\ell_1$  optimization problem. (d) The pixels used in the CS reconstruction are shown in white and are randomly distributed. (e) An interpolation from the samples using Delaunay triangulation. (f) Line scans from the line indicated in red on images (a-c,e).

magnetic force microscopy. In these settings, the tip is typically moved from point to point along a regular grid, engaging the tip at each point and either measuring the force curve, or measuring the height and then withdrawing to measure the magnetic response. Since the measurements already involve the approach and withdraw process, the CS approach will reduce the measurement time by exactly the fraction of measurements acquired.

#### IV. SIMULATIONS

To illustrate the CS approach, simulations with two samples were performed. The first sample was a grating provided by the Altug lab at Boston University. The grating was imaged in contact mode using an Agilent 5500 with a resolution of  $128 \times 128$  pixels (see Fig. 1a). The grating was a regular pattern that filled the entire image. The image was imported into Matlab and a random collection of 20% of the pixels was sampled. An image of the same size as the original was then reconstructed using either the relaxed  $\ell_1$  problem in (4) (shown in Fig. 1c) or a variant of the TV (gradient based)-problem as in (5) but with relaxed constraints to account for noise in the measurements (shown in Fig. 1b). Both algorithms were solved using the solvers in the  $\ell_1$  Magic collection [28]. The pixels used in both reconstructions are shown in Fig. 1d. Note that since the sampling for the CS

approach was done in Matlab based on the original image, there were no dynamics involved in the measurement process and thus we do not have an equivalent imaging time.

While the  $\ell_1$ -based reconstruction is clearly poor, the TV-based reconstruction does a good job at recovering the image. The primary error is found on the edges and likely arises from a small instability due to the size of the gradient filter implemented in  $\ell_1$  Magic. Away from the edges, the reconstruction clearly captures both the edges and the relatively flat areas of the sample. This is particularly clear from the line scan (at the indicated line in each of the reconstructions) shown in Fig. 1f.

While the CS approach produces a good image, the optimization step is computationally intensive. A rational alternative to building an image based on a nonraster collection of data is to interpolate the results. As a comparison, then, we created an interpolated image based on Delaunay triangulation, shown in Fig. 1e. While the grating is easily discernible, the image is clearly of lower quality than the reconstruction in Fig. 1b, especially with respect to high spatial frequencies.

Finally, we also considered for comparison a smooth sampling pattern represented by a spiral scan as illustrated in Fig. 2a. In practice one might use a circular spiral (as in [29]) but since the data was already given as a collection of pixels,

the square pattern was adopted. While such a scan pattern is likely to be coherent with respect to the image and thus to not satisfy the conditions in CS for accurate reconstruction, the path is easy for the tip to follow and the scan times are directly reduced by the reduction in total scan length. Note that the total number of pixels sampled along the scan pattern was again 20% of the original 16,384 samples.

An image, shown in Fig. 2b, was reconstructed from the samples using the gradient-based variant. While the reconstructed image is good in the center, the edges of the image are much poorer than in the randomly sampled case.

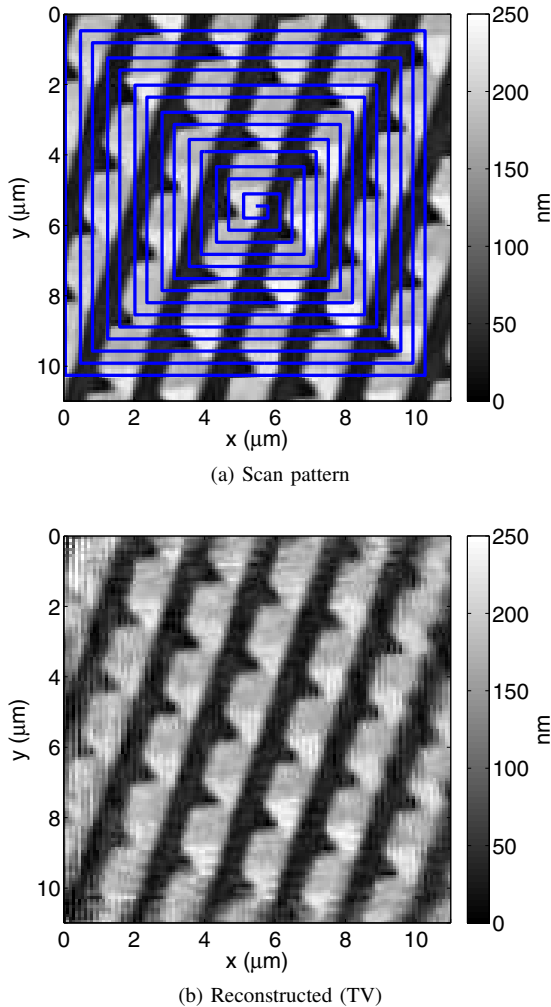


Fig. 2. Grating sample results using a spiral scan with 20% of the original pixels based on spiral scan. (a) The spiral scan superimposed on the original image. (b) The reconstruction based on the modified TV-problem.

The second example is based on an AFM image of DNA. The original image, shown in Fig. 3a, was acquired using an Asylum Research MFP-3D in intermittent contact (tapping) mode. Unlike the grating, this sample is visually sparse since most of the image is of substrate. As before, the image was imported into Matlab, a random sampling of pixels was chosen (shown in Fig. 3d), and two reconstructions were performed. A Delaunay triangulation based on the data was also created (shown in Fig. 3e).

Despite the sparsity of the sample, the results are quite similar to the grating example. The TV-based image is visually quite good, though the instability in the gradient filter is more predominant, due perhaps to the fact that the sample height is much smaller than with the grating. The  $\ell_1$ -based image is still poor, though the rough outline of the DNA is visible. The Delaunay triangulation is also reasonable, though it blurs the image significantly.

## V. CONCLUSION

In this paper we have described a CS approach to AFM imaging. Using a random sampling of pixels across the sample, a good reconstruction of the image can be created using only a small fraction of total pixels desired. While the need to engage and withdraw the tip of the instrument at every measurement location leads to a total sampling time that is roughly equivalent to a fast-AFM raster scan, the method allows for much less interaction with the sample and lower forces through optimized engaging. Furthermore, when applied to applications such as force mapping, the scheme can yield significant reductions in imaging time.

## ACKNOWLEDGEMENTS

This work was supported in part by the NSF under grants CMMI-0700877 and CMMI-0845742 as well as by a grant from Agilent Technologies. The authors also thank Daniel Abramovitch of Agilent Technologies and Paul Barbone of Boston University for helpful discussions of these ideas. They also thank Hatice Altug of Boston University for providing the grating sample.

## REFERENCES

- [1] D. Y. Abramovitch, S. B. Andersson, L. Y. Pao, and G. Schitter, "A tutorial on the mechanisms, dynamics and control of atomic force microscopes," in *Proc. American Control Conference*, 2007, pp. 3488–3502.
- [2] G. Schitter and M. J. Rost, "Scanning probe microscopy at video-rate," *Materials Today*, vol. 11, no. 1-2, pp. 40–48, January-February 2008.
- [3] M. B. Viani, T. E. Schäffer, G. T. Palocz, L. I. Pietrasanta, B. L. Smith, J. B. Thompson, M. Richter, M. Rief, H. E. Gaub, K. W. Plaxco, A. N. Cleland, H. G. Hansma, and P. K. Hansma, "Fast imaging and fast force spectroscopy of single biopolymers with a new atomic force microscope designed for small cantilevers," *Rev. Sci. Instr.*, vol. 70, no. 11, pp. 4300–4303, November 1999.
- [4] K. K. Leang and A. J. Fleming, "High-speed serial-kinematic AFM scanner: design and drive considerations," *Asian J. Contr.*, vol. 11, no. 2, pp. 144–153, March 2009.
- [5] G. Schitter, K. Astrom, B. DeMartini, P. Thurner, K. Turner, and P. Hansma, "Design and modeling of a high-speed AFM-scanner," *IEEE Trans Contr. Syst. Tech.*, vol. 15, no. 5, pp. 906–915, September 2007.
- [6] A. J. Fleming and K. K. Leang, "Charge drives for scanning probe microscope positioning stages," *Ultramicroscopy*, vol. 108, no. 12, pp. 1551–1557, 2008.
- [7] G. M. Clayton, S. Tien, and K. K. Leang, "A review of feedforward control approaches in nanopositioning for high-speed SPM," *J. Dyn. Sys. Meas. Contr.*, vol. 131, no. 6, p. 061101 (19 pages), 2009.
- [8] J. A. Butterworth, L. Y. Pao, and D. Y. Abramovitch, "Adaptive-delay combined feedforward/feedback control for raster tracking with applications to AFMs," in *Proc. American Control Conference*, 2010, pp. 5738–5744.
- [9] S. M. Salapaka, A. Sebastian, J. P. Cleveland, and M. V. Salapaka, "High bandwidth nano-positioner: A robust control approach," *Rev. Sci. Instr.*, vol. 73, no. 9, pp. 3232–3241, September 2002.

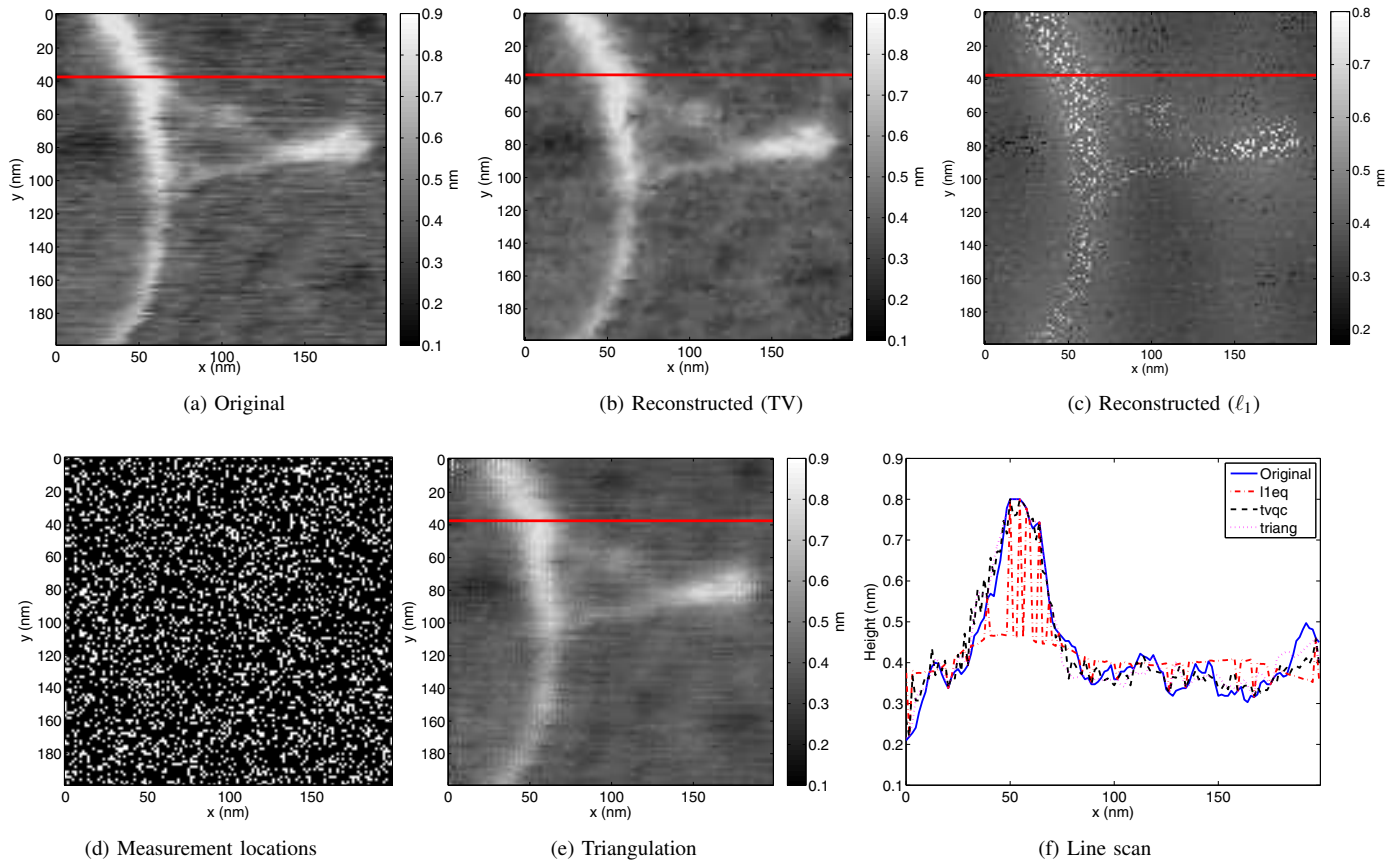


Fig. 3. DNA sample results using 20% of the pixels. (a) The full raster-scan image is sparse as the DNA occupies only a small portion of the scanned region. (b) Reconstruction using the relaxed TV optimization problem (see Sec. II-B). (c) Reconstruction using the relaxed  $\ell_1$  optimization problem. (d) The pixels used in the CS reconstruction are shown in white and are randomly distributed. (e) An interpolation from the samples using Delaunay triangulation. (f) Line scans from the line indicated in red on images (a-c,e).

- [10] S. Tien, Q. Zou, and S. Devasia, "Iterative control of dynamics-coupling-caused errors in piezoscanners during high-speed AFM operation," *IEEE Trans. Contr. Syst. Tech.*, vol. 13, no. 6, pp. 921–931, November 2005.
- [11] P. I. Chang, P. Huang, J. Maeng, and S. B. Andersson, "Local raster scanning for high speed imaging of biopolymers in atomic force microscopy," *Rev. of Sci. Instr.*, vol. no. 6, 063703 (7 pages), 2011.
- [12] E. Candés, "Compressive sampling," in *International Congress of Mathematics*, 2006, pp. 1433–1452.
- [13] B. Song, N. Xi, R. Yang, K. W. C. Lai, and C. Qu, "Video rate atomic force microscopy (AFM) imaging using compressive sensing," in *Proc. IEEE International Conference on Nanotechnology*, 2011, pp. 1056–1059.
- [14] J. Ma, "Compressed sensing for surface characterization and metrology," *IEEE Trans. Instrum. Meas.*, vol. 59, no. 6, pp. 1600–1615, June 2010.
- [15] M. H.-M. Cheng, G. T.-C. Chiu, and R. Reifengerger, "Fractal compression and adaptive sampling: reducing the image acquisition time in scanning probe microscopy," *Scanning*, vol. 30, pp. 463–473, 2008.
- [16] R. Baraniuk, "Compressive sensing," *IEEE Signal Proc. Mag.*, vol. 24, no. 4, pp. 118–121, July 2007.
- [17] M. A. Davenport, M. F. Duarte, Y. C. Eldar, and G. Kutyniok, *Compressed Sensing: Theory and Applications*. Cambridge University Press, 2011, ch. 1. Introduction to Compressed Sensing.
- [18] R. A. DeVore, "Nonlinear approximation," *Acta Numerica*, vol. 7, pp. 51–150, 1998.
- [19] E. Candés, J. Romberg, and T. Tao, "Robust uncertainty principles: exact signal reconstruction from highly incomplete frequency information," *IEEE Trans. Info. Theory*, vol. 52, no. 2, pp. 489–509, February 2006.
- [20] R. G. Baraniuk, M. A. Davenport, R. A. DeVore, and M. B. Wakin, "A simple proof of the restricted isometry property for random matrices," *Constructive Approximation*, vol. 28, no. 1, pp. 253–263, 2008.
- [21] M. L. Workman, R. L. Kosut, and G. F. Franklin, "Adaptive proximate time-optimal servomechanisms: continuous time case," in *Proc. American Control Conference*, 1987, pp. 589–594.
- [22] L. Y. Pao and G. F. Franklin, "Proximate time-optimal control of third-order servomechanisms," *IEEE Trans. Auto. Contr.*, vol. 38, no. 4, pp. 560–580, April 1993.
- [23] Z. Shen and S. B. Andersson, "Minimum time control of a second order system," in *IEEE Conference on Decision and Control*, 2010, pp. 4819–4824.
- [24] J. A. Butterworth, L. Y. Pao, and D. Y. Abramovitch, "Dual-adaptive feedforward control for raster tracking with applications to AFMs," in *Proc. Multi-Conference on Systems and Control*, 2011.
- [25] G. Schitter and A. Stemmer, "Identification and open-loop tracking control of a piezoelectric tube scanner for high-speed scanning-probe microscopy," *IEEE Trans. Contr. Systems Technology*, vol. 12, no. 3, pp. 449–454, May 2004.
- [26] G. Schitter, A. Stemmer, and F. Allgower, "Robust 2DOF-control of a piezoelectric tube scanner for high speed atomic force microscopy," in *Proc. American Control Conference*, 2003, pp. 3720–3725.
- [27] J. Arthur Earl Bryson and Y.-C. Ho, *Applied Optimal Control: Optimization, Estimation, and Control*, 2nd ed. Hemisphere Publishing Corporation, 1975.
- [28] [Online]. Available: <http://users.ece.gatech.edu/justin/l1magic/>
- [29] I. A. Mahmood, S. R. Moheimani, and B. Bhikkaji, "A new scanning method for fast atomic force microscopy," *IEEE Trans. Nanotech.*, vol. 10, no. 2, pp. 203–216, March 2011.